

# The concept of effective tension for fluctuating vesicles

U. Seifert\*

Institut für Festkörperforschung, Forschungszentrum Jülich, D-52425 Jülich, Germany

Received: 18 August 1994 / Revised version: 15 November 1994

**Abstract.** Vesicles are closed surfaces of bilayer membranes. Their mean shapes and fluctuations are governed by the competition of curvature energy and geometrical constraints on the enclosed volume and total surface area. A scheme to calculate these fluctuations to lowest order in the ratio of temperature to bending rigidity is developed. It is shown that for fluctuations that break a symmetry of the mean shape the area constraint indeed acts like a tension whose value is given by the Lagrange multiplier used to enforce the area constraint in the first place. As a consequence, these fluctuations are also insensitive to the specific variants of the curvature model. For fluctuations that preserve the symmetry of the mean shape the role of the area constraint is more subtle. The low temperature expansion breaks down in the spherical limit where with the excess area another small parameter enters. By incorporating the area constraint in this limit exactly, the validity of the conventional approach using an effective tension for fluctuations of quasi-spherical vesicles can be assessed.

**PACS:** 05.40+j; 82.70-y

## 1. Introduction

Vesicles are large encapsulating bags of a lipid bilayer membrane which form spontaneously in aqueous environment due to the hydrophobic effect [1]. Video microscopy reveals an amazing variety of shapes among which shape transformations can be induced by changing parameters like the temperature or the osmotic conditions. These membranes are soft enough to allow for thermally excited fluctuations around these mean shapes to be visible under the microscope.

Interest in these systems from the statistical mechanics perspective arises from the fundamental difference between conformations of vesicles and those of liquid droplets. While

liquid interfaces are governed by surface tension, the conformations of vesicles are determined by both bending elasticity [2, 3, 4] and geometrical constraints on the total surface area and the enclosed volume. A vesicle has a constrained area due to the fact that there are basically no free lipid molecules in aqueous solution. Thus, the number of molecules in the membrane is fixed. This constraint implies that the area is fixed since stretching and compressing the membrane requires much more energy than bending. Likewise, due to the inevitable presence of osmotically active molecules in the aqueous solution, the volume of the vesicles is determined by the requirement that basically no osmotic pressure builds up [3].

For a calculation of the shape of lowest energy, these constraints are added with Lagrange multipliers to the curvature energy which arises from the bending elasticity. Minimization then yields indeed a large variety of shapes [5–8]. These shapes are organized into phase diagrams which consist of regions of shapes with a definite symmetry separated by shape transitions where the symmetry of a shape changes. Various variants of the curvature model have been investigated which differ in the way the bilayer aspect is treated. An example of both an experimentally observed shape transformation and theoretically calculated shapes is shown in Fig. 1 taken from [9].

At this stage, it seems that surface tension is a superfluous concept for vesicles. Their conformations rather live in the “conjugated” ensemble where the area is constrained. Still, there has been some confusion about surface tension of membranes mostly due to the lack of a sensible definition of surface tension in such a system. The folklore includes statements like “the surface tension vanishes due to the fact that each molecule has its preferred area” or “the surface tension is practically infinite since membranes are so hard to stretch.” While the former can be justified in the sense that the area can adjust optimally to its preferred value, the latter statement is nonsense even though membranes are comparatively hard to stretch indeed. Physical insight is contained in the idea that “the area constraint implies an ‘effective’ or ‘entropic’ tension for fluctuations” [10–12] but, for a non-spherical shape, there never has been given a precise quan-

Dedicated to Prof. Herbert Wagner on the occasion of his 60th birthday

\* New address: Max-Planck-Institut für Kolloid- und Grenzflächenforschung, Kantstrasse 55, D-14513 Teltow-Seehof, Germany

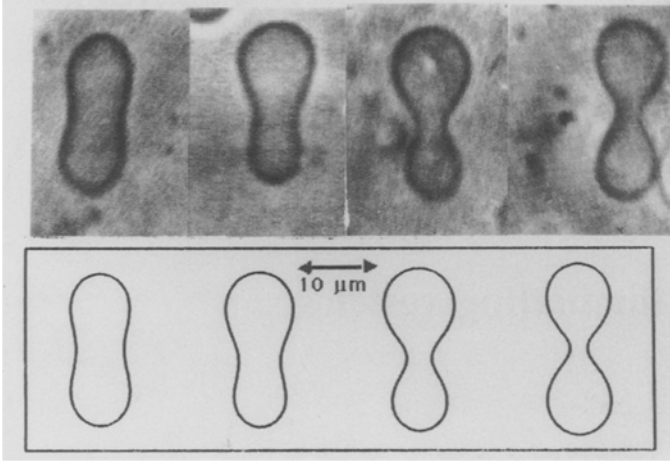


**Fig. 1.** Example of a shape transformation taken from Ref.[9]. The temperature is raised from left to right. The theoretical contours have been calculated within the BC model. All shapes are axisymmetric with respect to an axis from top to bottom. Moreover, the first and the last shape have reflection symmetry

tification of this tension let alone a prescription for how to calculate it.

For *almost planar* membranes the confusion around the notion of a surface tension has been clarified in [13] where the crucial role of the boundary conditions is shown. Quantitative theoretical work on fluctuations of *closed* vesicles, so far, has been almost exclusively devoted to the so-called *quasi-spherical* vesicles. Their fluctuation spectrum has been calculated using an “effective tension” as a Lagrange multiplier to mimic the area constraint [11]. The theoretical result has been used to analyse the experimentally observed flicker spectrum from which the bending rigidity can be obtained [14–19]. This theoretical approach demands further vindication since even though Lagrange multipliers are well established for implementing constraints for mean shapes, i.e., for calculations involving the first variation, there is no justification a priori to use them for the calculation of fluctuations (which involves the second variation) in a constrained ensemble. Fluctuations around *non-spherical* mean shapes have been investigated only by Peterson [20–24] who determines the fluctuations of vesicles with a shape similar to red blood cells in two variants of the curvature model. In his approach, the role of the constraints, however, is somewhat hidden in the formalism.

The purpose of this paper is to elucidate the role of an effective tension for *fluctuating vesicles*. In Sect. 3, we set up a scheme to calculate fluctuations for non-spherical vesicles taking into account the geometrical constraints. Even though no surface tension is introduced to begin with, our results for the fluctuations will lead to a natural interpretation in terms of an effective tension. The formalism is unifying in the sense that fluctuations are treated for any variant of the curvature model as introduced in Sect. 2. In particular, we prove that fluctuations that break a symmetry of the mean shape are insensitive to the variant of the curvature model. For these fluctuations the area constraint acts exactly like a tension whose value is given by the Lagrange multiplier used to enforce the area constraint when calculating the shape of

lowest energy. To the contrary, fluctuation that preserve the symmetry of the mean shape such as contour fluctuations of axisymmetric shapes do depend on the variant under consideration. For these fluctuations, an effective tension seems not to be a readily available concept.

The expansion parameter for thermal fluctuations is  $T/\kappa$ , where  $T$  is the temperature, Boltzmann’s constant is set to unity and  $\kappa$  is the bending rigidity. With the typical value  $\kappa = 10^{-19}J$ , one gets  $T/\kappa = 1/25$  at room temperature. This expansion breaks down in the spherical limit since, for a sphere, there is no area left for fluctuations. Formally, a second small parameter, the excess area, enters in this limit. In Sect. 4, we set up a scheme which allows again to treat the area constraint exactly in the spherical limit, in contrast to previous approaches using an effective tension. Our results together with a calculation of the relative area fluctuations within the conventional approach allow to determine the range of validity of the conventional treatment.

## 2. Stationary shapes in curvature models

### A. Variants of the curvature model

The energy of a vesicle arises from bending the membrane [2–4]. Since a typical linear extension of a vesicles is in the micron range while the membrane is only nanometers thick, a vesicle is described as a two-dimensional surface embedded in three dimensional space. Such a surface can locally be characterized by its mean curvature,  $H$ , and its Gaussian curvature,  $K$ , from which one obtains the bending energy as

$$\kappa G \equiv \kappa \frac{1}{2} \oint dA (2H)^2 \quad (1)$$

with the dimensionless “local” bending energy  $G$ . The integral over the Gaussian curvature  $K$ , which yields only a topological constant, is ignored. The energy  $\kappa G$  has to be augmented by constraints on both the total area of the vesicles

$$A \equiv 4\pi R_0^2, \quad (2)$$

which defines the length-scale  $R_0$ , and the enclosed volume  $V$ .

A minimal model for vesicle conformations then amounts to minimizing the energy  $\kappa G$  at constant area and volume. Due to the scale invariance of  $G$ , such a model depends only on the reduced volume

$$v \equiv \frac{V}{(4\pi/3)R_0^3} \leq 1, \quad (3)$$

(where equality holds for the sphere only). Analysis of this model has revealed [7] that pear like shapes with broken up/down symmetry as shown in Fig. 1 do not appear as stationary shapes in such a model. This indicates a posteriori that the minimal model lacks an essential feature which turns out to be a signature of the fact that the membrane is a bilayer rather than a symmetric monolayer. Over the last twenty years, three different ways have been suggested to include the bilayer aspect which leads to the different variants of the curvature model.

(i) *The spontaneous curvature (SC) model.* Helfrich [3] in a seminal paper introduced the energy

$$F_{SC} \equiv \frac{\kappa}{2} \oint dA (2H - C_0)^2 \equiv \kappa (G - 2C_0M + C_0^2 A/2), \quad (4)$$

Here,  $C_0$  is the so-called spontaneous curvature which is supposed to reflect a possible asymmetry in the membrane and

$$M \equiv \oint dAH \quad (5)$$

is the total (integrated) mean curvature.

(ii) *The bilayer couple (BC) model.* In a complementary approach, building on the earlier work by Evans [4, 25], Svetina and Zeks [26, 6] introduced the so-called bilayer couple (BC) model, in which a hard constraint on the area difference

$$\Delta A = 4dM + O(d^2) \quad (6)$$

between the neutral surfaces of the two monolayers, which are separated a distance  $2d$  from each other, is imposed. The physical justification of this constraint was believed to be the fact that the two monolayers do not exchange molecules. This was translated somewhat erroneously into a constraint on the area of each individual monolayer. Thus, this model is defined by the energy (1) together with the *three* constraints on area, volume and total mean curvature.

(iii) *The area-difference elasticity (ADE) model.* The derivation of the curvature model starting from a continuum elastic theory for each monolayer has shown that both of the above variants amount to limiting cases of a more general (and physically better justified) model. The energy of a vesicle in this area-difference elasticity model is given by [27–30]

$$\begin{aligned} W &\equiv \left( \oint dA (2H - C_0)^2/2 + \frac{\alpha}{2R_0^2} (M - M_0)^2 \right) \\ &= \kappa \left( G - 2C_0M + C_0^2 A/2 + \frac{\alpha}{2R_0^2} (M - M_0)^2 \right), \end{aligned} \quad (7)$$

Here,  $M_0$  is the scaled optimal area difference,

$$M_0 \equiv \frac{N^+ - N^-}{4\phi_0 d}, \quad (8)$$

which depends on both the number of molecules,  $N^+$  and  $N^-$ , of lipid molecules in each layer and their equilibrium density  $\phi_0$ . The applicable constraints are those on area and volume while the control parameters are  $C_0$  and  $M_0$ .

The last term in (7) is the so-called area-difference elasticity or non-local curvature energy. It arises from the fact that even though both monolayers do not exchange molecules on the experimentally relevant time-scales, small relative compression and expansion of the two leaflets is energetically comparable to the local bending energy. If one assumes that the monolayers are homogeneous sheets of thickness  $2d$ , one obtains for the dimensionless material parameter  $\alpha$  the estimate  $\alpha = 3/\pi \simeq 1$ , which is indeed supported by measurements [31, 32]. In the limit  $\alpha \rightarrow \infty$ , one recovers from the ADE model the BC model, while for  $\alpha = 0$  one ends up with the SC model.

## B. Stationary shapes

Vesicles will acquire the shape at which their curvature energy subject to the appropriate constraints is minimal. To find these shapes, first the set of *stationary shapes* is determined for which the first variation of the appropriate energy subject to the applicable constraints vanishes. This set includes local minima as well as saddle points which have, in principle, to be discarded by a stability analysis. To find the set of stationary shapes within the BC model consider the general variational free-energy

$$\Phi[S] = \kappa G[S] + \Sigma A[S] + PV[S] + QM[S], \quad (9)$$

where the dimensionless local curvature energy  $G$  has been defined in Eq. (1) and  $[S]$  denotes symbolically the dependence on the shape  $S$ . The parameters  $\Sigma$ ,  $P$  and  $Q$  are Lagrange multipliers for the fixed area, volume and mean curvature, respectively. The stationarity condition for the functional  $\Phi[S]$  formally reads

$$\delta^1 \Phi[S] = \kappa \delta^1 G[S] + \Sigma \delta^1 A[S] + P \delta^1 V[S] + Q \delta^1 M[S] = 0, \quad (10)$$

where  $\delta^1$  denotes the first variation. This formal shape equation becomes an ordinary non-linear differential equation if one restricts to axisymmetric shapes [5, 21, 6, 8, 7]. These equations have been solved systematically in [7], which leads to theoretical shapes as shown in Fig. 1. For any stationary shape, the Lagrange parameters fulfill the relations

$$\begin{aligned} \Sigma/\kappa &= -\frac{\partial G}{\partial A}|_{V,M}, \quad P/\kappa = -\frac{\partial G}{\partial V}|_{A,M}, \quad \text{and} \\ Q/\kappa &= -\frac{\partial G}{\partial M}|_{A,V}. \end{aligned} \quad (11)$$

The first relation shows that the Lagrange multiplier, or “tension”,  $\Sigma$  is minus the change of the bending energy with increasing area at both constant volume and total mean curvature. Depending on the specific shape, this quantity can have either sign.

For the SC model, the area constraint is added by a term  $\Sigma_{SC}$  to the energy  $F_{SC}$ . By setting

$$\Sigma = \Sigma_{SC} + \kappa C_0^2 \quad \text{and} \quad Q = -2\kappa C_0, \quad (12)$$

a stationary shape in the BC model becomes stationary in the SC model. Likewise, in the ADE model, one adds the area constraint by  $\Sigma_{ADE}$  to the energy  $W$ . Setting

$$\begin{aligned} \Sigma &= \Sigma_{ADE} + \kappa C_0^2/2 \quad \text{and} \\ Q &= -2\kappa C_0 + \alpha \kappa (M - M_0) \end{aligned} \quad (13)$$

any stationary shape from the BC model becomes stationary for the ADE model. The set of stationary shapes thus is the same in all variants of the curvature model [7, 30]. At fixed reduced volume  $v$ , there is typically a one parameter set of stationary shapes within each symmetry class. However, the local stability of a shape can depend on the variant. For the shapes shown in Fig. 1, the stability can be checked by inspection of the energy bifurcation diagram [30]. It turns out that the pears with weak up/down asymmetry are stable within the ADE model for large  $\alpha$ , and, thus, in particular within the BC model. Likewise, pears with the weak up/down asymmetry become unstable for small  $\alpha$  and within the SC model. The question then arises how the fluctuation spectrum depends on the variant of the curvature model or on  $\alpha$ . This issue will be addressed next.

### 3. Gaussian fluctuations with constraints

#### A. Formalism

In this subsection, we set up an expansion of the fluctuations around the stationary shape in the small parameter  $T/\kappa$ . The fluctuating shape can be parametrized by

$$\mathbf{R}(s_1, s_2) = \mathbf{R}_0(s_1, s_2) + \epsilon(s_1, s_2)\mathbf{n}(s_1, s_2), \quad (14)$$

where  $\mathbf{n}(s_1, s_2)$  is the local normal vector and  $s_{1,2}$  are internal coordinates. The quantities of interest are both the thermal shift of the mean shape  $\langle \epsilon(s_1, s_2) \rangle$ , which will be shown not to vanish, and correlation functions like  $\langle \epsilon(s_1, s_2)\epsilon(s'_1, s'_2) \rangle$ . The bracket  $\langle \dots \rangle$  denotes the appropriate thermal average and will be defined below.

The local normal displacement  $\epsilon(s_1, s_2)$  is expanded,

$$\epsilon(s_1, s_2) = \sum_i a_i \epsilon_i(s_1, s_2), \quad (15)$$

in a set of basis functions  $\{\epsilon_i\}$ . For axisymmetric vesicles, the spherical harmonics

$$\epsilon_i(s_1, s_2) \equiv Y_{l,m}(s\pi/s^*, \phi). \quad (16)$$

with  $a_{l,-m} = (-1)^m a_{l,m}^*$  are a convenient basis [21]. Here,  $s^*$  is the length of the contour from north pole to south pole. The formal index  $i$  has thus become a double index  $(l, m)$  and the  $\sum_i$  is defined as

$$\sum_i \equiv \sum_{l=0}^{l_{\max}} \sum_{m=-l}^l \quad (17)$$

with some upper cutoff  $l_{\max}$ . This leads to a total number of modes

$$N = \sum_{l=0}^{l_{\max}} \sum_{m=-l}^l = (l_{\max} + 1)^2. \quad (18)$$

In order not to overburden the notation we will keep the short hand notation with just one index  $i$ . The expansion based on Eqs. (15) and (16) can deal with any axisymmetric stationary shape, whether it is star-shaped or not. In particular, this expansion is not restricted to nearly spherical shapes.

We will first consider the fluctuations in the BC model, the other cases then becoming trivial modifications. The geometrical quantities area, volume, mean curvature as well as the bending energy  $G$  can be expanded in the set  $\{a_i\}$ . Formally, one thus obtains

$$G = G_0 + g_i a_i + (1/2) a_i G_{ij} a_j + O(a_i^3), \quad (19)$$

$$A = A_0 + R_0^2 \left( d_i^{(1)} a_i + (1/2) a_i D_{ij}^{(1)} a_j + O(a_i^3) \right), \quad (20)$$

$$V = V_0 + R_0^3 \left( d_i^{(2)} a_i + (1/2) a_i D_{ij}^{(2)} a_j + O(a_i^3) \right), \quad (21)$$

and

$$M = M_0 + R_0 \left( d_i^{(3)} a_i + (1/2) a_i D_{ij}^{(3)} a_j + O(a_i^3) \right). \quad (22)$$

Here, and from now on, summation over double indices will be understood. Specifically for axisymmetric vesicles, the quantities  $g_i, G_{ij}, d_i^\alpha$  and  $D_{ij}^\alpha$  can be expressed as integrals over the contour. The integrands are quantities such as the

local curvature and Legendre polynomials and derivatives thereof. The specific expressions are lengthy [33] and will not be needed for the general discussion to follow.

Since  $\mathbf{R}_0(s_1, s_2)$  is a stationary shape at constant area, volume and mean curvature, enforced by the Lagrange multipliers  $\Sigma, P$  and  $Q$ , we have from Eq.(10) for all  $i$

$$\kappa g_i + \Sigma R_0^2 d_i^{(1)} + P R_0^3 d_i^{(2)} + Q R_0 d_i^{(3)} = 0. \quad (23)$$

Thermal expectation values are now defined as

$$\langle h\{a_i\} \rangle \equiv \frac{1}{Z} \int \mathcal{D}\{a_i\} \delta\left(\frac{A - A_0}{R_0^2}\right) \delta\left(\frac{V - V_0}{R_0^3}\right) \times \delta\left(\frac{M - M_0}{R_0}\right) \exp\left(\frac{-\kappa(G - G_0)}{T}\right) h\{a_i\}. \quad (24)$$

with the partition function

$$Z \equiv \int \mathcal{D}\{a_i\} \delta\left(\frac{A - A_0}{R_0^2}\right) \delta\left(\frac{V - V_0}{R_0^3}\right) \times \delta\left(\frac{M - M_0}{R_0}\right) \exp\left(\frac{-\kappa(G - G_0)}{T}\right). \quad (25)$$

The crucial issue is to define the measure  $\mathcal{D}\{a_i\}$ , which should physically correspond to an integration over all surfaces near the stationary shape, not counting any surface twice. We will argue in Appendix A that the naive measure

$$\int \mathcal{D}\{a_i\} \equiv \prod_{l=0}^{l_{\max}} \left( \prod_{m=0}^l \int_{-\infty}^{\infty} \frac{d\Re(a_{l,m})}{\sqrt{2\pi}} \right) \times \left( \prod_{m=1}^l \int_{-\infty}^{\infty} \frac{d\Im(a_{l,m})}{\sqrt{2\pi}} \right). \quad (26)$$

is sufficient to the low order  $T/\kappa$ , in which we work. It is convenient to introduce a generating functional

$$Z(\{J_i\}) \equiv \int \mathcal{D}\{a_i\} \delta\left(\frac{A - A_0}{R_0^2}\right) \times \delta\left(\frac{V - V_0}{R_0^3}\right) \delta\left(\frac{M - M_0}{R_0}\right) \times \exp\left(\frac{-\kappa(G - G_0)}{T}\right) \exp(J_i a_i), \quad (27)$$

from which correlation functions can be obtained by simple derivatives such as

$$\langle a_i \rangle = \partial_{J_i} \ln Z|_{\{J_i=0\}} \quad (28)$$

and

$$\langle a_i a_j \rangle = \partial_{J_i} \partial_{J_j} \ln Z|_{\{J_i=0\}}. \quad (29)$$

The essential step is to write the three  $\delta$ -functions in (24) as Fourier integrals in the form

$$\delta(x) = \exp\left(\frac{-\kappa \lambda^\alpha x}{T}\right) \int_{-\infty}^{\infty} \frac{dk^\alpha}{2\pi} \exp(ik^\alpha x) \quad (30)$$

where  $\alpha = 1, 2, 3$  (no summation on  $\alpha!$ ) and the set of scaled Lagrange multipliers  $\{\lambda^\alpha\}$  is defined as  $\lambda^1 \equiv \Sigma/\kappa$ ,  $\lambda^2 \equiv P/\kappa$  and  $\lambda^3 \equiv Q/\kappa$ , respectively. The prefactor in front of the integral in (30) will compensate the linear term  $g_i a_i$  when inserted into the generating functional (27). For small  $T/\kappa$ , it will be sufficient to use the expansions (19-22) up

to quadratic order in  $a_i$ . Inserting these expansions into the generating functional, one gets

$$Z(\{J_i\}) = \int \mathcal{D}\{a_i\} \left[ \prod_{\gamma=1}^3 \int_{-\infty}^{\infty} \frac{dk^\gamma}{2\pi} \right] \times \exp \left( -\frac{\kappa}{2T} a_i (S_{ij} - \frac{T}{\kappa} i k^\alpha D_{ij}^\alpha) a_j \right) \times \exp \left( (i k^\beta d_i^\beta + J_i) a_i \right). \quad (31)$$

Here, the *stability matrix*  $\mathbf{S}$  with matrix elements

$$S_{ij} \equiv G_{ij} + \lambda^\alpha D_{ij}^\alpha \quad (32)$$

is obtained from the second variation of both the curvature energy and the geometrical constraints.

To set up a perturbation theory, it is useful to note that  $a_i \sim (T/\kappa)^{1/2}$ ,  $k^\alpha \sim (T/\kappa)^{-1/2}$ , and  $J_i \sim (T/\kappa)^{-1/2}$  which follows from the fact that generically both  $S_{ij}$  and  $d_i$  are of order 1. Since we are interested in small  $T/\kappa$  we can thus expand the first exponential in the expression (31) and write it in the form

$$\exp \left( -\frac{\kappa}{2T} a_i (S_{ij} - \frac{T}{\kappa} i k^\alpha D_{ij}^\alpha) a_j \right) \approx \exp \left( -\frac{\kappa}{2T} a_i S_{ij} a_j \right) \times \left( 1 + i \frac{1}{2} k^\alpha \partial_{J_m} D_{mn}^\alpha \partial_{J_n} \right). \quad (33)$$

It can be checked a posteriori that higher order terms in this expansion do not contribute at the low order  $T/\kappa$ .

If the stability matrix  $\mathbf{S}$  is positive definite, the Gaussian integrals over the  $\{a_i\}$  in (31) can be performed easily. This leads to

$$Z(\{J_i\}) = \frac{1}{\det^{1/2} \mathbf{S}} \left[ \prod_{\alpha=1}^3 \int_{-\infty}^{\infty} \frac{dk^\alpha}{2\pi} \right] \times \left( 1 + i \frac{1}{2} k^\alpha \partial_{J_m} D_{mn}^\alpha \partial_{J_n} \right) \times \exp \left( \frac{T}{2\kappa} (i k^\beta d_i^\beta + J_i) S_{ij}^{-1} (i k^\gamma d_j^\gamma + J_j) \right). \quad (34)$$

In fact, a slight complication arises here from the presence of trivial zero-modes associated with rigid motion of the shape [34]. The solution of how to overcome this more technical issue is discussed in Appendix A. Finally, we perform the Gaussian integrals over the  $k^\alpha$  which yields

$$Z(\{J_i\}) = \frac{1}{\det^{1/2} \mathbf{S}} \frac{1}{\det^{1/2} \mathbf{W}} \frac{1}{(2\pi)^{3/2}} \times \left( 1 - \frac{1}{2} \partial_{J_m} \partial_{J_n} D_{mn}^\alpha (W^{\alpha\beta})^{-1} d_p^\beta S_{ps}^{-1} J_s \right) \times \exp \left( \frac{T}{2\kappa} J_i C_{ij} J_j \right). \quad (35)$$

The matrix  $\mathbf{W}$  with elements

$$W^{\alpha\beta} \equiv d_i^\alpha S_{ij}^{-1} d_j^\beta. \quad (36)$$

is a  $3 \times 3$  matrix with respect to the Greek indices. The correlation matrix  $\mathbf{C}$  has elements

$$C_{ij} \equiv \left( S_{ij}^{-1} - d_k^\alpha S_{ik}^{-1} W^{\alpha\beta-1} S_{jl}^{-1} d_l^\beta \right). \quad (37)$$

## B. Correlation functions

If the generating functional (35) is inserted into (29), the correlation functions of the amplitudes  $\{a_i\}$  are obtained as

$$\langle a_i a_j \rangle = \frac{T}{\kappa} C_{ij} = \frac{T}{\kappa} \left( S_{ij}^{-1} - d_k^\alpha S_{ik}^{-1} W^{\alpha\beta-1} S_{jl}^{-1} d_l^\beta \right). \quad (38)$$

In order to discuss this expression from a general perspective, it is useful to classify the set of modes  $\{\epsilon_i\}$  according to their symmetry properties. We will call those modes *symmetry breaking modes* that break a symmetry of the stationary shape. For an axisymmetric vesicle, all modes with index  $m \neq 0$  belong to the symmetry breaking modes. If, moreover, the stationary shape possesses reflection symmetry, as the first and the fourth shape of Fig. 1 do, the modes with  $m = 0$  and  $l$  uneven belong to this class too. By symmetry, the first variation in the geometrical quantities and the bending energy vanishes identically for these modes, i.e.  $d_i^\alpha = g_i = 0$ . The remaining *symmetry preserving modes* do not change the symmetry of the mean shape and will, thus, in general, have linear terms  $d_i^\alpha \neq 0$  and  $g_i \neq 0$ .

The stability matrix  $\mathbf{S}$  factors in these two classes and, moreover, within each class in different subclasses according to the symmetry of the respective modes. In particular, for an axisymmetric mean shape with reflection symmetry, the modes with different index  $|m|$  do not mix, and neither do those with different parity but the same  $|m|$ . Therefore, one can discuss the correlations of these two classes of modes separately.

For the *symmetry breaking modes*, we find from (38) the simple result

$$\langle a_i a_j \rangle = \frac{T}{\kappa} S_{ij}^{-1} \quad (39)$$

for the correlation function, which is remarkable for the following reason. Suppose, we had calculated the correlation function for the same stationary shape in the  $\Phi$ -ensemble (9) in which the terms  $\Sigma A + PV + QM$  count as “real” energies assuming that the “fields”  $\Sigma, P$  and  $Q$  are external parameters. For fluctuations in the  $\Phi$ -ensemble, we would have obtained exactly the result (39) since the stability matrix  $\mathbf{S}$  is nothing but the second variation of the energy  $\Phi$ , compare Eq.(32). Thus, the correlations of all symmetry breaking modes do not depend on whether one imposes hard constraints or whether one considers the term  $\Sigma A + PV + QM$  as contributing to the energy. This result has profound consequences for the interpretation of the Lagrange multipliers  $\Sigma, P$  and  $Q$ . In particular, one can consider  $\Sigma$  as a tension restricting (or promoting, depending on its sign) the fluctuations.

However, the equivalence of the fluctuations in the BC model and the  $\Phi$ -ensemble is not complete since for all modes which preserve the axisymmetry, i.e., in particular, for fluctuations of the contour of an axisymmetric vesicle, the additional term in (37) shows that fluctuations in the constrained ensemble are different from those where the  $\Sigma A + PV + QM$ -term is treated as a real energy. This distinction in the correlation function between modes that break a symmetry and those that do not is a central result of this approach.

### C. Thermal shift of the mean shape

The modes that do not break a symmetry of the stationary shape acquire a finite temperature shift to make up for the area – and, strictly speaking, also for the volume and the mean curvature – stored in the fluctuating modes. If (35) is inserted into (28), one obtains

$$\langle a_i \rangle = -\frac{T}{\kappa} d_k^\alpha W^{-1\alpha\beta} D_{mn}^\beta (2S_{kn}^{-1} C_{mi} + S_{ki}^{-1} C_{mn}). \quad (40)$$

This expression yields the shift in the mean shape as

$$\langle \mathbf{R}(s_1, s_2) \rangle = \mathbf{R}_0(s_1, s_2) + \sum_i \langle a_i \rangle \epsilon_i(s_1, s_2) \mathbf{n}(s_1, s_2). \quad (41)$$

For an axisymmetric vesicle, this expression can be reduced to a shift of the mean contour, since  $\sum_i$  includes contributions from the ( $m=0$ )-modes only. The thermal shift is of order  $T/\kappa$  and thus much smaller than a typical fluctuation, which scales as  $a_i \sim (T/\kappa)^{1/2}$ .

### D. Results for other variants

The formalism and the discussion of the results have been set up within the BC model. A strength of the approach introduced here is its flexibility with which it can be used to discuss mean shape shifts and correlations in the other variants of the curvature model.

For the SC model, there are only two constraints but a different energy. Technically speaking, this amounts to replacing  $G$  by  $G - 2C_0 M + C_0^2 A/2$  which entails the replacements

$$g_i \rightarrow g_i - 2C_0 R_0 d_i^{(3)} + (C_0 R_0)^2 d_i^{(1)}/2 \quad (42)$$

and

$$G_{ij} \rightarrow G_{ij} - 2C_0 R_0 D_{ij}^{(3)} + (C_0 R_0)^2 D_{ij}^{(1)}/2. \quad (43)$$

Since the Lagrange multipliers are accordingly changed as given in (11), the stability matrix occurring in (31) remains exactly the one given in (32). Therefore, the correlation functions of the symmetry breaking modes for the SC-model are exactly the same as in the BC-model. For the symmetry preserving modes, both the fluctuations and the mean shape shifts are still given by (38) and (40), respectively. However, the sums over Greek indices run only through 1 and 2 leading to different numerical values.

For the ADE model, the energy  $G$  has to be replaced by  $G - 2C_0 M + C_0^2 A/2 + (\alpha/2R_0^2)(M - M_0)^2$ . With the corresponding changes in the quantities  $g_i$  and  $G_{ij}$ , one finds for the stability matrix the replacement

$$S_{ij} \rightarrow S_{ij} + \alpha d_i^{(3)} d_j^{(3)}. \quad (44)$$

With this modification, the results (40) and (38) for the mean shape shift and the correlation function still holds, with Greek indices running only through 1 and 2. Since  $d_i^{(3)} = 0$  for all symmetry breaking modes, the correlation functions for these modes are again identical to those in the BC-model. *The difference between the various ensembles shows up only in the correlations involving symmetry preserving modes.*

### E. Stability

So far, we have implicitly assumed that the stationary shape is locally stable with respect to the deformations as parametrized by the expansion (15) once the Euclidean modes are excluded. Of course, the same approach also leads to a stability criterion which can be read off from the correlation matrix  $\mathbf{C}$  defined in Eq. (38). Due to the presence of constraints the matrix  $\mathbf{C}$  has to have three zero eigenvalues for the BC model and two zero eigenvalues for those variants where only two hard constraints are imposed. These eigenvalues always show up in the class of symmetry preserving modes. If, moreover, the correlation matrix has negative eigenvalues, the shape is unstable.

Two cases of negative eigenvalues of the correlation matrix must be distinguished. If the negative eigenvalue arises within the modes which break a symmetry, the stability matrix already exhibits this negative eigenvalue. Such a shape will be unstable with respect to the corresponding eigenvector in all variants of the curvature model. *Thus, stability with respect to a deformation that breaks a symmetry does not depend on the variant of the curvature model.* This has been observed previously for a particular shape within the SC and the BC model in [24].

If the negative eigenvalue of  $\mathbf{C}$  arises within the modes which keep the symmetry of the shapes, then the stability of this particular shape indeed depends on the specific variant of the curvature model. An example are the pears with the weak asymmetry shown as the second and third shape in Fig. 1, which are unstable for small  $\alpha$  and become stable for larger  $\alpha$  [30].

### F. Spherical limit

As the mean shape around which the expansion has been performed approaches the sphere, the fluctuations should become smaller since for a sphere as stationary shape, there is no area available for fluctuations at constant volume. In the approach outlined above, the modes with different  $l$  no longer mix in this limit. Therefore, the correlation matrix is given by the inverse of the stability matrix  $\mathbf{S}$ , which leads in the spherical limit to

$$\langle |a_{l,m}|^2 \rangle \approx \frac{T}{\kappa} \frac{1}{(l+2)(l-1)(l^2+l-6)} \quad (45)$$

for all variants of the curvature model.

This expression diverges for the  $l=2$ -mode which points to an inconsistency. In fact, in the spherical limit a second small parameter,  $1-v$ , arises, which invalidates the naive expansion in  $T/\kappa$ .

## 4. Quasi-spherical vesicles

### A. Expansion around the sphere

The spherical limit has to be analysed within a different approach, which allows to keep track of both small parameters,  $T/\kappa$  and  $1-v$ . The fluctuating shape is not expanded

around the corresponding stationary shape but rather around a sphere with the same volume

$$V \equiv \frac{4\pi}{3} R_V^3, \quad (46)$$

which defines  $R_V$ . We consider a fixed area

$$A \equiv (4\pi + \Delta) R_V^2, \quad (47)$$

which defines the (dimensionless) excess area  $\Delta$  used as a small parameter instead of  $1 - v$ .

A quasi-spherical vesicle can be parametrized by spherical harmonics

$$R(\theta, \phi) = R_V \left( 1 + \sum_{l \geq 2} \sum_{m=-l}^l u_{l,m} Y_{lm}(\theta, \phi) \right), \quad (48)$$

where  $|m| \leq l$  and  $u_{l,-m} = (-1)^m u_{l,m}^*$ . Expanding the geometrical quantities as well as the bending energy around a sphere, one has [35, 11, 36]

$$G = 8\pi + \frac{1}{2} \sum_{l \geq 1} \sum_{m=-l}^l |u_{l,m}|^2 (l+2)(l+1)l(l-1) + O(u_{l,m}^3), \quad (49)$$

$$A = R_V^2 \left( 4\pi \left( 1 + \frac{u_{0,0}}{\sqrt{4\pi}} \right)^2 + \sum_{l \geq 1} \sum_{m=-l}^l |u_{l,m}|^2 (1 + l(l+1)/2) + O(u_{l,m}^3) \right), \quad (50)$$

and

$$V = R_V^3 \left( \frac{4\pi}{3} \left( 1 + \frac{u_{0,0}}{\sqrt{4\pi}} \right)^3 + \sum_{l \geq 1} \sum_{m=-l}^l |u_{l,m}|^2 + O(u_{l,m}^3) \right). \quad (51)$$

The volume constraint (46) fixes the amplitude  $u_{0,0}$  as a function of the other amplitudes

$$u_{0,0} = - \sum_{l \geq 1} \sum_{m=-l}^l |u_{l,m}|^2 / \sqrt{4\pi}, \quad (52)$$

where we truncate from now on the cubic terms. If this value is inserted into (50), the area constraint (47) becomes

$$\sum_{l \geq 1} \sum_{m=-l}^l |u_{l,m}|^2 \frac{(l+2)(l-1)}{2} = \Delta \quad (53)$$

Since the  $(l = 1)$ -modes correspond to translations, which have to be omitted, from now on all sums start at  $l = 2$ . It is convenient to absorb both the  $l$ -dependence of the area term and a factor  $T/\kappa$  into the amplitudes by defining

$$v_{l,m} \equiv u_{l,m} \left( \frac{\kappa}{T} \frac{(l+2)(l-1)}{2} \right)^{1/2}. \quad (54)$$

We also define the ratio  $\tau$  between reduced temperature and excess area as

$$\tau \equiv \frac{T}{\kappa \Delta}. \quad (55)$$

## B. Exact treatment of the area constraint

We determine the amplitudes in the minimal model since the other variants of the curvature model lead to the same results at the level considered here as shown in Appendix B. The mean-square amplitudes  $\langle |v_{l,m}|^2 \rangle$  then follow from the constraint (53) and the Boltzmann factor with the energy  $G$  as [37]

$$\begin{aligned} \langle |v_{l,m}|^2 \rangle &= \frac{1}{Z} \int \mathcal{D}\{v_{l,m}\} \delta \left( \sum_{l \geq 2} \sum_{m=-l}^l |v_{l,m}|^2 - 1/\tau \right) \\ &\quad \times |v_{l,m}|^2 \exp \left( - \sum_{l \geq 2} \sum_{m=-l}^l p_l |v_{l,m}|^2 \right) \\ &= - \frac{1}{(2l+1)} \frac{\partial}{\partial p_l} \ln Z. \end{aligned} \quad (56)$$

The factor  $1/(2l+1)$  in (56) arises from the degeneracy of the energy with respect to  $m$ . After performing the derivative,  $p_l$  has to be set to

$$p_l \equiv l(l+1). \quad (57)$$

The partition function  $Z$  is defined as

$$\begin{aligned} Z &\equiv \int \mathcal{D}\{v_{l,m}\} \delta \left( \sum_{l \geq 2} \sum_{m=-l}^l |v_{l,m}|^2 - 1/\tau \right) \\ &\quad \times \exp \left( - \sum_{l \geq 2} p_l |v_{l,m}|^2 \right) \end{aligned} \quad (58)$$

with the discretized functional integral

$$\begin{aligned} \int \mathcal{D}\{v_{l,m}\} &\equiv \prod_{l=2}^{l_{\max}} \left( \prod_{m=0}^l \int_{-\infty}^{\infty} \frac{d\Re(v_{l,m})}{\sqrt{2\pi}} \right) \\ &\quad \times \left( \prod_{m=1}^l \int_{-\infty}^{\infty} \frac{d\Im(v_{l,m})}{\sqrt{2\pi}} \right). \end{aligned} \quad (59)$$

Without the constraint, the partition function would be a trivial Gaussian integral. Introducing the usual Fourier transformation for the  $\delta$ -function,  $\delta(x) = \int_{-\infty}^{\infty} (d\lambda/2\pi) e^{-i\lambda x}$ , the integrals over the  $v_{l,m}$  become Gaussian and can easily be performed. Thus one obtains

$$Z = \int_{-\infty}^{\infty} \frac{d\lambda}{2\pi} e^{i\lambda/\tau} \prod_{l \geq 2}^{l_{\max}} (p_l + i\lambda)^{-(l+1/2)}. \quad (60)$$

In principle, this one-dimensional integral could be analysed numerically. However, as shown below, the approximations made by ignoring higher order terms in (49)–(51) are consistent only for small and for large  $\tau$ . In both cases, an analytical calculation of  $Z$  is possible as follows.

For  $\tau \ll 1$ , i.e. for  $T/\kappa \ll \Delta$ , the integral can be treated by a saddle-point-like approach. First, one applies Cauchy's theorem and closes the path of integration in the upper complex  $\lambda$  half-plane. The integrand has branch-cuts originating at  $\lambda = ip_l$ , which we choose parallel to the positive real- $\lambda$ -axis. For small  $\tau$ , only the singularity with the smallest

imaginary part, which is the branch-cut along  $\lambda = ip_2 + \epsilon$ , contributes. The integral around this branch leads to

$$Z = \frac{8}{3} \frac{\partial^2}{\partial p_2^2} \left[ e^{-p_2/\tau} \int_0^\infty d\epsilon e^{i\epsilon/\tau} (i\epsilon)^{-1/2} \times \prod_{l \geq 3}^{l_{\max}} (p_l - p_2 + i\epsilon)^{-(l+1/2)} \right] \left[ 1 + O(e^{-(g_3 - p_2)/\tau}) \right]. \quad (61)$$

For small  $\tau$ , the integral yields

$$Z \approx \frac{8}{3} \frac{\partial^2}{\partial p_2^2} \left[ e^{-p_2/\tau} \Gamma(1/2) \tau^{1/2} \prod_{l \geq 3}^{l_{\max}} (p_l - p_2)^{-(l+1/2)} \right]. \quad (62)$$

Inserting this into Eq.(56) and expressing the result in terms of the amplitudes  $u_{l,m}$  leads to

$$\langle |u_{l,m}|^2 \rangle = \frac{T}{\kappa} \left[ \frac{1}{(l+2)(l-1)(l^2+l-6)} + O(\tau) \right] \quad (63)$$

for  $l \geq 3$  and

$$\langle |u_{l,m}|^2 \rangle = \frac{\Delta}{5} \left[ \frac{1}{2} - \tau \sum_{l \geq 3} \frac{2l+1}{(l+2)(l-1)(l^2+l-6)} + O(\tau^2) \right] \quad (64)$$

for  $l = 2$ .

The leading term for  $l \geq 3$  is exactly what we found in Sect. 3.F in the spherical limit. Thus, the direct evaluation of the correlation functions in the spherical limit shows that the procedure described in Sect. 3.F holds (for  $l \geq 3$ ) in the double limit  $\Delta \rightarrow 0$  after  $T/\kappa \rightarrow 0$ . In addition, the leading term for the amplitude for the ( $l = 2$ )-modes is obtained correctly. These modes pick up most of the excess area. Of course, the distribution of this area among the five ( $l = 2$ )-modes cannot be obtained in the quadratic approximation. Note also that the area constraint is obeyed exactly as the second order contribution in (64) shows.

In principle, one could continue the expansions (63) and (64) to higher orders in  $\tau$ . However, this would lead to misleading results since the terms which have been omitted in the quadratic expansions (49)–(51) are more relevant than those higher order terms. Consider, e.g., the omitted terms of the form  $u_{2,m}^{2n} u_{4,m'}^2$  with  $n \geq 1$  which are of the order  $\Delta^n T/\kappa$ . In the limit  $\tau \rightarrow 0$ , such a term is not small compared to  $(T/\kappa)\tau$ , which are the next to leading order term in (63). In order to improve the values given in (63) one would thus have to include all terms of the form  $u_{2,m}^{2n} u_{4,m'}^2$ , i.e. one would have to expand around the stationary shape rather than around the sphere.

For  $\tau \gg 1$ , i.e. for  $\Delta \ll T/\kappa$ , integrating over the  $u_{l,m}$  is not so convenient. Inspection of (56) shows that in this case the bending energy can be treated as small perturbation. The zero order term is defined by the partition function

$$Z_0 \equiv \int \mathcal{D}\{v_{l,m}\} \delta \left( \sum_{l \geq 2} \sum_{m=-l}^l |v_{l,m}|^2 - 1/\tau \right) \quad (65)$$

In lowest order, all  $v_{l,m}$  thus have the same amplitude  $\langle |v_{l,m}|^2 \rangle = 1/(\tau N)$ , which leads to

$$\langle |u_{l,m}|^2 \rangle \approx \frac{2\Delta}{N(l+2)(l-1)}. \quad (66)$$

In this regime, all  $N$  modes share the available excess area as previously observed in [11]. Corrections to this result are for the order  $1/\tau$  and can be obtained by expanding the exponential in (56) and performing the averages with  $Z_0$ . In the limit  $\Delta \rightarrow 0$ , i.e. for  $\tau \rightarrow \infty$ , the fluctuations vanish. However, one then enters a different physical regime in which the stretching of the membrane must be taken into account.

In summary, the analysis given in this section shows that an analytical calculation of the fluctuations of quasi-spherical vesicles taking into account the area constraint exactly is possible for large and small  $\tau$ . An expansion beyond the leading term for small  $\tau$  does not fail due to the absence of an analytical scheme but rather due to the relevance of the higher order terms in the expansions (49)–(51).

### C. Conventional approach with effective tension

We now discuss the conventional approach to fluctuations in the quasi-spherical limit [14, 11, 17]. First, in these works the relevance of the higher order terms in the expansions (49)–(51) are tacitly neglected. Therefore, in this respect, this approach inevitably suffers from the same deficiencies as the approach discussed above. Secondly, the area constraint is not treated by introducing a  $\delta$ -function in the partition function (58) but rather by a Lagrange multiplier which requires further justification.

We discuss this approach here for the minimal model since the other variants lead to the same result as shown in Appendix B. The mean-square amplitudes in this approach are calculated with the Boltzmann factor

$$\exp \left( -(\kappa G + \bar{\Sigma} A)/T \right), \quad (67)$$

where the “tension”  $\bar{\Sigma}$  is another, yet free, Lagrange multiplier to be distinguished by the over-bar from the Lagrange multiplier  $\Sigma$  used in calculating the stationary shape. After inserting the quadratic expansions (49)–(51) into energy and area, with  $u_{0,0}$  replaced by the volume constraint (52), one obtains

$$\kappa G + \bar{\Sigma} A \approx \text{const} + \frac{\kappa}{2} \sum_{l \geq 2} \sum_{m=-l}^l |u_{l,m}|^2 (l+2)(l-1) \times ((l+1)l + \bar{\sigma}), \quad (68)$$

with the dimensionless effective tension

$$\bar{\sigma} \equiv \bar{\Sigma} R_V^2 / \kappa. \quad (69)$$

If this expression is used as a Boltzmann weight for the amplitudes  $\{u_{l,m}\}$ , one immediately obtains the mean square amplitudes

$$\langle |u_{l,m}|^2 \rangle = \frac{T}{\kappa} \frac{1}{(l+2)(l-1)((l+1)l + \bar{\sigma})}. \quad (70)$$

These expressions for the mean square amplitudes have been used to determine experimentally the bending rigidity  $\kappa$  from the contour fluctuations of quasi-spherical vesicles using phase contrast microscopy combined with fast image



processing [14–19]. In this approach,  $\bar{\sigma}$  is usually either set to 0 or treated as a fit parameter for which one typically obtains values in the range  $0 \lesssim \bar{\sigma} \lesssim 100$ . This effective tension is also called an *entropic* tension [10, 11, 12] since it can be interpreted as arising from restricting (at least for  $\bar{\sigma} > 0$ ) the fluctuations of the individual modes by the area constraint.

Since the Lagrangian multiplier  $\bar{\Sigma}$  has been introduced only to enforce the area constraint, it should, in fact, be eliminated in favor of the excess area  $\Delta$  which is the physically meaningful quantity. Inserting the mean square amplitudes (70) into the expansion of the area and comparing with the constraint (47) yields an implicit equation [37],

$$\sum_{l=2}^{l_{\max}} \frac{2l+1}{l^2+l+\bar{\sigma}(\Delta)} = \frac{2\Delta\kappa}{T} = \frac{2}{\tau}, \quad (71)$$

for  $\bar{\sigma}$ . An analogous relation was first derived for almost planar membranes [10]. The relation (71) shows that  $\bar{\sigma}$  depends on the excess area only in the combination  $\Delta\kappa/T = 1/\tau$ . Thus, after elimination of the effective tension, the mean square amplitudes as given by (70) depend only on the three quantities,  $T/\kappa$ ,  $\tau$ , and the cutoff  $l_{\max}$ .

In general, (71) has to be inverted numerically to yield  $\bar{\sigma} = \bar{\sigma}(\tau, l_{\max})$ . It is instructive to discuss limit cases analytically. For small  $\tau$ , one finds

$$\bar{\sigma} \approx -6 + \frac{5}{2}\tau + O(\tau^2). \quad (72)$$

Inserting this value into (70), one recovers the exact limits (63) and (64). However, the next to leading order terms in an expansion in  $\tau$  of either (70) or (63) do *not* coincide.

The fact that the effective tension is negative for small  $\tau$  may look strange at first sight, but becomes clear in view of the relation (11). In fact,  $\Sigma R_0^2/\kappa = -6$  is also the spherical limit of the (dimensionless) Lagrange multiplier for prolate and oblate ellipsoids. The effective tension for fluctuations is negative, thus promoting fluctuations, because if area is taken up by the fluctuations with  $l \geq 3$ , the curvature energy stored in the ( $l=2$ )-modes decreases. For  $l \geq 3$ , the fluctuations with area constraint are thus larger than without an area constraint which shows again that one should interpret the effective tension quite carefully.

For large  $\tau$ , one obtains from (71)

$$\bar{\sigma} \approx \frac{\tau}{2} l_{\max}^2, \quad (73)$$

which after insertion into the mean square amplitudes again coincides with the exact limit (66).

If the inversion of (71) is performed analytically by replacing the sum with an integral, one obtains the exponential dependence of the tension on the excess area

$$\bar{\sigma} \approx \frac{l_{\max}^2 + l_{\max} - 6e^{2/\tau}}{e^{2/\tau} - 1}. \quad (74)$$

For intermediate values of  $\tau$  in the range  $2 \gg \tau \gg 1/\ln l_{\max}$ , one thus finds

$$\bar{\sigma} \approx l_{\max}^2 e^{-2/\tau}. \quad (75)$$

The consistency of this approach where the area constraint is treated by a Lagrange multiplier can be checked by calculating the fluctuations  $\delta\Delta$  in the dimensionless excess area defined as

$$\delta\Delta \equiv \frac{(\langle\Delta^2\rangle - \Delta^2)^{1/2}}{\Delta} = \frac{\tau}{\sqrt{2}} \left( \sum_l \frac{2l+1}{(l^2+l+\bar{\sigma}(\tau))^2} \right)^{1/2}. \quad (76)$$

For this quantity, one obtains in the three regimes

$$\delta\Delta \approx \begin{cases} \sqrt{2/5}, & \tau \ll 1/\ln l_{\max} \\ \frac{\tau}{\sqrt{2N}} e^{1/\tau}, & 1/\ln l_{\max} \ll \tau \ll 2, \\ \sqrt{2/N}, & 2 \ll \tau \end{cases}, \quad (77)$$

where we recall  $N \approx l_{\max}^2$  for large  $l_{\max}$ .

Taken at face value, this is a disturbing result. Only for small excess area, the fluctuations show the  $\sim 1/\sqrt{N}$  behavior characteristic of large systems. For large and intermediate excess area, the relative area fluctuations are larger and become of order 1 for  $\tau \lesssim 1/\ln l_{\max}$ . However, we have seen above that the approach with the effective tension yields the correct result in the limit  $\tau \rightarrow 0$ . The apparent discrepancy arises from the area fluctuations stored in the  $l=2$  modes. If those are neglected by restricting the sum in (76) to  $l \geq 3$ , one obtains, for  $\tau \lesssim 1/\ln l_{\max}$ ,  $\delta\Delta = O(\tau)$ , which is consistent with the finding that in the limit  $\tau \rightarrow 0$  the approach with the effective tension yields the correct result. The fluctuations that lead to  $\delta\Delta = O(1)$  are those of the ( $l=2$ )-modes for which the approach with the effective tension fails in order  $T/\kappa$  as shown above.

Experimentally, the crucial range is not quite  $\tau \rightarrow 0$  but rather  $\tau$  small but finite, say  $\tau \simeq 1/\ln l_{\max}$ . In this regime, the relative area fluctuations are of the size  $\delta\Delta = O(\tau)$  which may become about 10% for  $l_{\max} = 1000$ . One would expect that the amplitudes of the low lying modes then carry a similar error. How large the error actually is could be determined by calculating the integral (60) numerically and then comparing the results with the conventional approach. A first step towards such a comparison for  $l_{\max} = 20$  has been performed by a Monte Carlo simulation in [37] in a quite narrow  $\tau$  range. However, one should always keep in mind that neglecting higher order terms in the expansions (49)–(51) adds additional errors of the order  $\tau$ . To include those effects would require an expansion in (49)–(51) beyond the quadratic order [36]. At some point, these tedious calculations have to be done if one wants to extract from the analysis of quasi-spherical vesicle fluctuations both a high precision measurement of the bending rigidity and information as to which variant of the curvature model applies.

## 5. Summary

A unifying approach to treat fluctuations of vesicles subject to geometrical constraints was introduced. The main results include a distinction of fluctuations which break the symmetry of the mean shape from those which do not. For the former fluctuations, which are identical among all variants of curvature models, the area constraint acts exactly like an effective tension whose value is determined by the value of the Lagrange multiplier used to determine the mean shape. For the latter fluctuations, the role of the constraints is more subtle.

In the spherical limit, the exact approach outlined here vindicates a posteriori the conventional treatment by means

of an effective tension in two limiting cases. For the experimentally interesting parameter range of the ratio  $\tau$  of reduced temperature to excess area small but finite, the calculation of area fluctuations in the conventional approach indicates that the effective tension is an approximation which fails at order  $\tau$ . How severe this failure is needs to be clarified by further numerical work.

I thank M. Nikolic for working on the numerical implementation of the theory developed here. Stimulating discussion with her as well as with H.-G. Döbereiner, R. Lipowsky, E. Sackmann, and M. Wortis are gratefully acknowledged. M. Kraus' comments on a previous version and J. Krug's critical reading of this manuscript have been most helpful.

## Appendix A: remarks on the measure

The correct definition of a measure related to a fluctuating fluid membrane is a delicate problem [38–42]. The purpose of this section, which draws strongly on the illuminating works [39] and [40], is to present the evidence that the naive measure used in (26) yields the correct results for the correlation function (38) and the thermal shift (40) to the low order  $T/\kappa$ , in which we work.

Defining a measure for the integration over surfaces requires a discretization. While one could use a grid of size  $a$  in real space, any expansion in basis functions usually resembles more to a Fourier representation. The appropriate generalization of a Fourier transformation on the stationary shape are the eigenfunctions  $\{\hat{\epsilon}_i\}$  of the Laplace-Beltrami operator. If the set of these eigenfunctions  $\{\hat{\epsilon}_i\}$  are cut-off at an eigenvalue of the order of  $1/a^2$ , this set should provide a reasonable basis for an expansion of the normal displacement  $\epsilon(s_1, s_2)$ .

In defining a measure for the expansion coefficients  $\hat{a}_i$  of a normal displacement in the basis  $\{\hat{\epsilon}_i\}$ , one has to avoid over-counting surfaces which are the same except for reparametrization. This problem is tackled in [40] in some detail. It is shown that in the normal gauge we are using here, the Fadeev-Popov factor  $\mathcal{F}$ , which takes care of this reparametrization, can be expanded as  $\mathcal{F} = 1 + \text{const} \times \epsilon^2$ . This expansion leads to  $\mathcal{F}(\hat{a}_i) = 1 + \hat{\mathcal{F}}_{ij} \hat{a}_i \hat{a}_j$ , where the matrix elements  $\hat{\mathcal{F}}_{ij}$  depends on the stationary shape.

Thus, at this stage, the proper measure to be used in Eqs. (24) and (25) would have been

$$\int \mathcal{D}\{\hat{a}_i\} \equiv \prod_{i=1}^N \int_{-\infty}^{\infty} \frac{d\hat{a}_i}{\sqrt{2\pi}} \left(1 + \hat{\mathcal{F}}_{ij} \hat{a}_i \hat{a}_j\right). \quad (\text{A1})$$

Since it is convenient to stick with the basis  $\{\epsilon_i\}$ , one should express this measure in terms of the  $\{a_i\}$  which yields

$$\int \mathcal{D}\{\hat{a}_i\} = \mathcal{J} \prod_{i=1}^N \int_{-\infty}^{\infty} \frac{da_i}{\sqrt{2\pi}} (1 + \mathcal{F}_{ij} a_i a_j). \quad (\text{A2})$$

Here,  $\mathcal{J}$  is the Jacobian for the linear transformation from  $\{\hat{\epsilon}_i\}$  to  $\{\epsilon_i\}$  and  $\mathcal{F}_{ij}$  arises from  $\hat{\mathcal{F}}_{ij}$  by the appropriate transformation. The crucial point is that using this measure (A2) instead of (26) does not change the results (38) and (40) in lowest order  $T/\kappa$ . First, the Jacobian  $\mathcal{J}$  is just a number since  $\{\hat{\epsilon}_i\}$  and  $\{\epsilon_i\}$  are related by a linear transformation.

Secondly, the Fadeev-Popov factor yields only a higher order correction as can be verified easily.

Apart from the Fadeev-Popov factor, it is stressed in [40] that there is another correction to the measure which arises from the fact that the displaced surface has, in general, a different area than the original surface and thus superficially more (or less) degrees of freedom. For an arbitrary surface, this so-called Liouville factor, which restores the original degrees of freedom, has not yet been calculated in normal gauge. Still, it is clear that this factor cannot modify the correlation functions (38) to this order in  $T/\kappa$ . Less obvious is its effect on the thermal shifts (40). Since we keep the area of the fluctuating surface constant, one could expect that the Liouville factor does not modify the shifts either but a formal proof of this statement has to be left for future work [43].

Finally, we comment on the fact that due to Euclidean invariance several trivial zero modes appear in the expansion (15). For a generic shape, there are three translations and three rotations which leave the shape invariant [21]. These modes should rather not be included in the functional integral (26) from the outset. In practice, one can diagonalize the stability matrix  $\mathbf{S}$  where these modes show up as  $N_e = 5$  or 6 zero modes depending on whether or not the shape is axisymmetric.

The functional integral (26) should thus be replaced by

$$\int \mathcal{D}\{a_i\} \rightarrow \int \mathcal{D}\{\tilde{a}_i\} \equiv \tilde{\mathcal{J}} \prod_{i=1}^{N-N_e} \int_{-\infty}^{\infty} \frac{d\tilde{a}_i}{\sqrt{2\pi}}. \quad (\text{A3})$$

Here, the set  $\{\tilde{a}_i\}$  are the expansion coefficients with respect to a basis  $\{\tilde{\epsilon}_i\}$  of eigenvectors of the stability matrix  $\mathbf{S}$ . The product runs only over those modes which do not belong to the Euclidean zero eigenvalues of  $\mathbf{S}$ . Again the Jacobian,  $\tilde{\mathcal{J}}$ , is an irrelevant number. In this new basis, quantities like  $g_i, G_{ij}, d_i^\alpha$  and  $D_{ij}^\alpha$  should acquire a tilde too. We assume that from Eq.(33) onwards this change of basis has been tacitly performed and that the tildes have been dropped to keep the notation simple.

## Appendix B: equivalence of all variants in the spherical limit

We finally show that all variants of the curvature model are equivalent in the spherical limit. The other variants differ from the minimal model in the respective energy  $B$ , which can be written for the spherical limit in the form

$$B = \kappa G + g(A, M), \quad (\text{B1})$$

with an obvious  $g(A, M)$ . The expansion of the mean curvature  $M$  in the spherical limit reads

$$\begin{aligned} M &= R_V \left( 4\pi \left( 1 + \frac{u_{0,0}}{\sqrt{4\pi}} \right) + \sum_{l \geq 1} \sum_{m=-l}^l |u_{l,m}|^2 l(l+1)/2 \right) \\ &= R_V \left( 4\pi + \sum_{l \geq 2} \sum_{m=-l}^l |u_{l,m}|^2 (l+2)(l-1)/2 \right). \end{aligned} \quad (\text{B2})$$

For the latter relation, we fixed  $u_{0,0}$  by the volume constraint (52). Once this is done, the expansion of the mean curvature

turns out to be proportional to the expansion of the area (50). This fact lies behind the equivalence of the ensembles in the spherical limit. The expansion of the total energy  $B$  now reads with  $A_V \equiv 4\pi R_V^2$  and  $M_V \equiv 4\pi R_V$

$$B - 8\pi\kappa - g(A_V, M_V) = \frac{\kappa}{2} \sum_{l \geq 2}^{l_{\max}} \sum_{m=-l}^l |u_{l,m}|^2 (l+2)(l-1) \times (l(l+1) + \bar{\sigma}_B), \quad (\text{B3})$$

with

$$\bar{\sigma}_B \equiv \frac{R_V^2}{\kappa} \frac{\partial g}{\partial A} \Big|_{(A=A_V, M=M_V)} + \frac{R_V}{\kappa} \frac{\partial g}{\partial M} \Big|_{(A=A_V, M=M_V)}. \quad (\text{B4})$$

For the calculation of the fluctuations in the spherical limit as in Sect. 4.B, the only modification for the other variants will thus be a constant shift in the quantities  $p_l$  which will be defined for the other variants by

$$p_l \equiv l(l+1) + \bar{\sigma}_B. \quad (\text{B5})$$

Such a shift of  $p_l$ , however, does not affect the results for the mean square amplitudes. Likewise, in the conventional approach using  $\bar{\Sigma}$  to ensure the area constraint, the effective tension in (69) will be defined as

$$\bar{\sigma} \equiv \bar{\Sigma} R_V^2 / \kappa + \bar{\sigma}_B. \quad (\text{B6})$$

Since the Lagrange multiplier  $\bar{\Sigma}$  has no independent physical significance in this approach and the amplitudes depend only on the effective tension  $\bar{\sigma}$ , the details of the variant of the curvature model do not effect any of the results. This fact has a merit and a drawback. The merit is that the fluctuations of quasi-spherical vesicles are universal in the sense that they depend only on the local bending rigidity, the temperature and the excess area which should make the analysis of experimental data simpler. On the other hand, this universality shows that one can not expect to decide on a specific variant of the curvature model on the basis of the conventional analysis of quasi-spherical fluctuations. This universality has independently been shown within the ADE model in [32].

## References

1. For reviews, see (a) R. Lipowsky, *Nature* **349**, 475 (1991); (b) M. Wortis, U. Seifert, K. Berndl, B. Fourcade, L. Miao, M. Rao, and R. Zia, in *Dynamical phenomena at interfaces, surfaces and membranes*, edited by D. Beysens, N. Boccarda, and G. Forgacs (Nova Science, New York, 1993), pp. 221–236; (c) U. Seifert and R. Lipowsky, in *Handbook of Physics of Biological Systems*, vol. 1, edited by R. Lipowsky and E. Sackmann (Elsevier, Amsterdam 1994).
2. P. Canham, *J. Theoret. Biol.* **26**, 61 (1970).
3. W. Helfrich, *Z. Naturforsch.* **28c**, 693 (1973).
4. E. Evans, *Biophys. J.* **14**, 923 (1974).
5. H. Deuling and W. Helfrich, *J. Physique* **37**, 1335 (1976).
6. S. Svetina and B. Zeks, *Eur. Biophys. J.* **17**, 101 (1989).
7. U. Seifert, K. Berndl, and R. Lipowsky, *Phys. Rev. A* **44**, 1182 (1991).
8. L. Miao, B. Fourcade, M. Rao, M. Wortis, and R. Zia, *Phys. Rev. A* **43**, 6843 (1991).
9. K. Berndl, J. Käs, R. Lipowsky, E. Sackmann, and U. Seifert, *Europhys. Lett.* **13**, 659 (1990).
10. W. Helfrich and R.-M. Servuss, *Il Nuovo Cimento* **3D**, 137 (1984).
11. S. Milner and S. Safran, *Phys. Rev. A* **36**, 4371 (1987).
12. E. Evans and W. Rawicz, *Phys. Rev. Lett.* **64**, 2094 (1990).
13. F. David and S. Leibler, *J. Phys. II France* **1**, 959 (1991).
14. M. Schneider, J. Jenkins, and W. Webb, *J. Phys.* **45**, 1457 (1984).
15. H. Engelhardt, H. Duwe, and E. Sackmann, *J. Physique Lett.* **46**, L 395 (1985).
16. I. Bivas, P. Hanusse, P. Bothorel, J. Lalanne, and O. Aguerre-Chariol, *J. Phys.* **48**, 855 (1987).
17. J. Faucon, M. Mitov, P. Meleard, I. Bivas, and P. Bothorel, *J. Phys. France* **50**, 2389 (1989).
18. H. Duwe, J. Käs, and E. Sackmann, *J. Phys. France* **51**, 945 (1990).
19. P. Meleard, J. Faucon, M. Mitov, and P. Bothorel, *Europhys. Lett.* **19**, 267 (1992).
20. M. Peterson, *J. Math. Phys.* **26**, 711 (1985).
21. M. Peterson, *J. Appl. Phys.* **57**, 1739 (1985).
22. M. Peterson, *Mol. Cryst. Liq. Cryst.* **127**, 159 (1985).
23. M. Peterson, H. Strey, and E. Sackmann, *J. Phys. II France* **2**, 1273 (1992).
24. M. Peterson, *Phys. Rev. A* **45**, 4116 (1992).
25. E. Evans, *Biophys. J.* **30**, 265 (1980).
26. S. Svetina and B. Zeks, *Biochimica et Biophysica Acta* **42**, 86 (1983).
27. U. Seifert, L. Miao, H.-G. Döbereiner, and M. Wortis, in *The Structure and Conformation of Amphiphilic Membranes*, Vol. 66 of *Springer Proceedings in Physics*, edited by R. Lipowsky, D. Richter, and K. Kremer (Springer, Berlin, 1991), pp. 93–96.
28. W. Wiese, W. Harbich, and W. Helfrich, *J. Phys.: Cond. Matter* **4**, 1647 (1992).
29. B. Bozic, S. Svetina, B. Zeks, and R. Waugh, *Biophys. J.* **61**, 963 (1992).
30. L. Miao, U. Seifert, M. Wortis, and H.-G. Döbereiner, *Phys. Rev. E* **49**, 5389 (1994).
31. R. Waugh, J. Song, S. Svetina, and B. Zeks, *Biophys. J.* **61**, 974 (1992).
32. A. Yeung, Ph.D. thesis, University of British Columbia, 1994.
33. M. Nikolic, U. Seifert, and M. Wortis, in preparation.
34. M. Peterson, *Phys. Rev. A* **39**, 2643 (1989).
35. W. Helfrich, *J. Physique* **47**, 321 (1986).
36. Z.-C. Ou-Yang and W. Helfrich, *Phys. Rev. A* **39**, 5280 (1989).
37. I. Bivas, L. Bivolarski, M. Mitov, and A. Derzhanski, *J. Phys. II* **12**, 1423 (1992).
38. W. Helfrich, *J. Physique* **48**, 285 (1987).
39. P. Nelson and T. Powers, *J. Phys. II France* **3**, 1535 (1993).
40. W. Cai, T. Lubensky, P. Nelson, and T. Powers, *J. Phys. II France* **4**, 931 (1994).
41. D. Morse and S. Milner, *Europhys. Lett.* **26**, 565 (1994).
42. D. Morse and S. Milner, *Statistical Mechanics of Finite Fluid Membranes*, preprint, 1994.
43. I thank D. Morse, T. Lubensky and P. Nelson for illuminating discussions on the Liouville factor.